Journal of Geophysical Research Atmospheres

Supporting Information for

Predicting Frigid Mixed-Phase Clouds for Pristine Coastal Antarctica

Keith M. Hines[1], David H. Bromwich[1,2], Israel Silber[3], Lynn M. Russell[4], and Lesheng Bai[1]

[1]Polar Meteorology Group, Byrd Polar & Climate Research Center, The Ohio State University, Columbus, Ohio 43210

[2]Atmospheric Sciences Program, Department of Geography, The Ohio State University, Columbus, Ohio 43210

[3]Department of Meteorology and Atmospheric Sciences, The Pennsylvania State University, University Park, PA, 16802

[4]Scripps Institution of Oceanography, University of California San Diego, La Jolla, CA, 92093

Contents of this file

1 Map of McMurdo, Antarctica and vicinity

Figure S1 shows McMurdo Stations and regional features including Ross Island, the Ross Ice Shelf, and the Transantarctic Mountains. McMurdo is on the southern tip of Ross Island on a peninsula. There is considerable topography on Ross Island including Mount Erebus with a peak at 3794 m. The Transantarctic Mountains rise to over 3000 m to the west. McMurdo is very close to Ross Ice Shelf. Open water allows sea access to McMurdo for much of the year. Automatic weather station sites are shown by red triangles.

2 Polar WRF domains

Our simulations have two domains (Fig. S2). The outer domain has 10-km grid spacing and was identical to the Antarctic Mesoscale Prediction System (AMPS) grid 2 as of 2016. The nested grid has 2-km grid spacing and provides improved resolution of Ross Island and vicinity.

3 Surface and 500 hPa fields from AMPS

Figure 3 displays simulated near-surface atmospheric fields during these time periods for AMPS grid 3. Shown are sea level pressure contours, 2-m air temperature, and the 10-m wind barbs for the two cases. Contours are removed over higher topography. Simulations have two domains. The regional flow patterns are strongly influenced by the low local topography. Ross Island has robust local topography including Mt. Erebus with a summit of 3794 m. (Fig. S1b). Monaghan et al. (2005) found that the complex topography near McMurdo causes cloud occurrence to depend upon wind direction. Cold low-level airstreams are apparent, consistent with the pattern of the Ross Ice Shelf airstream described by Seefeldt and Cassano (2012). The wind flow usually has a southerly component over the very cold elevated terrain of East Antarctica, while southeast of McMurdo, southerly katabatic winds flow off the Ross Ice Shelf onto the Ross Sea. McMurdo, shown by the star in Fig. S3, is in the highly variable flow between these airstreams The two times shown during March 2016 (0600 UTC 08 March and 0600 UTC 11 March) show complicated mesoscale flow patterns (Figs. S3a and S3b). There are mesoscale circulations present with wind shear and considerable baroclinity in the region The near surface temperatures during March over the Ross ice Shelf are below -20°C, with warmer air over the Ross Sea to the north. Large temperature gradients are frequently near McMurdo. For the November case, a complicated low-level flow pattern is also present at 06000 UTC 09 November 2016 and 0600 UTC 12 November (Figs. S3c and S3d). Warmer temperatures are present over the Ross Ice Shelf and the Transantarctic Mountains than during the March case.

Figure S4 shows 500 hPa fields from AMPS grid 5 for the March and November test periods. AMPS grid 5 has 3.3-km grid spacing and is different than the model grids for this work. Figure S4 provides the middle tropospheric fields to correspond to the near-surface fields shown in Fig. S3. At 500 hPa there is a low near McMurdo at 0600 UTC on 11 March (Fig. S4b). For the November case, there is a trough with cyclonic (clockwise) turning in the region at 0600 UTC on 09 November that widens into a broader cyclonic feature on 0600 UTC 12 November (Figs. S4c and S4d). Therefore, the synoptic and mesoscale features may be favorable for cloud formation near Ross Island during the March and November study periods. The 500 hPa temperature field in Fig. S4 is not well-aligned with the 500 hPa contours, thus thermal advection is occurring. Accordingly, the synoptic and mesoscale structures are evolving during March and November cases, rather than a stable and slowly evolving equivalent barotropic structure. The cold

temperatures displayed in Figs. S3 and S4 are normally associated with small hydrometeor contents.

4 Vertical profiles of hydrometers for 13 November 2016

The vertical profiles in Fig. S5 are analogous to those shown in Fig. 6, but for the 24-hr averages on 13 November. The temperature and dewpoint temperature are close enough below 2500 m AGL in Fig. S5a that clouds may be present here. The dryer level above is not favorable for cloud formation. Figure S6c shows that the observed and simulated cloud fraction extend up to 3000 m. The Control simulation simulates some liquid water below 400 m (Figs. S5c and S5d), while some liquid fraction is observed below 1600 m, with a higher observed layer between 2500 – 3000 m. The cold bias as seen in Fig. S5a likely contributes to the simulated liquid cloud fraction seen in Fig. S5c below 400 m. The observing site is sometimes ice-free, but it is always permanent ice in the simulation. This difference may contribute to the cold bias. Another simulated layer of total cloud fraction extends from 1000 to 3000 m. Simulated ice water content is larger than the observed values above 1000 m (Fig. S5d), consistent with the simulated cloud fraction peaking near 2200 m, while the observed cloud fraction peaks near 700 m. Analogous to that shown by Fig. 6 for the March test period, the November test period has too much simulated ice and not enough simulated supercooled liquid water by the simulation ControlN.

5 Sensitivity tests with specified liquid droplet concentration

Section 4.3 detailed sensitivity tests to the ice microphysics in the P3 scheme. Here we include sensitivity tests to the specification of the liquid droplet concentration for the P3 scheme. The liquid cloud physics in P3 are one-moment, so the liquid droplet concentration is not calculated. The liquid droplet concentration was specified at the default P3 value 200 cm^{-3} for the Control simulation and the ice physics sensitivity tests. This number may be too large for the pristine conditions of coastal Antarctica. Liu et al. (2018) observed CCN concentrations at McMurdo, Antarctica over a range of supersaturations. We select the CCN concentrations at 1% supersaturation from Liu et al. (2018). For austral fall they found the mean CCN concentration at 1% supersaturation to be 132 cm^{-3}. The corresponding value for austral spring is 117 cm^{-3}. We apply these CCN values as the specified liquid droplet concentrations in simulations of the March and November cases, respectively. The ice microphysics settings are from the Vignon sensitivity tests. The new simulations called FallLiq and SpringLiq for the March and November cases, respectively, are listed in Table 1. For the March case, the new simulation was run for 7-11 March (Fig. S6a). The average liquid water path for 1200 UTC 7 March to 1200 UTC March 11 was 56.9 g m^{-2} for the observations, 47.9 g m^{-2} for Vignon, and 63.9 g m^{-2} for FallLiq. For November as shown in Fig. S6b, the corresponding liquid values for 0000 UTC 11 November to 0000 UTC 14 November were 17.8, 10.6, and

8.5 g m^{-2}, respectively. The change to a smaller liquid droplet number did not consistently increase or decrease the liquid water path. Instead, the liquid water path increased for March and decreased for November (Fig. S6). We find the sensitivity to the liquid droplet concentration for realistic values to be less than that to the ice physics in the P3 scheme.

6 Table of automatic weather stations for data assimilation

Table S1 shows the automatic weather stations (AWS) that are that provide observations every 3 hours for data assimilation. All the stations are in the vicinity of McMurdo Station. The data assimilation impacts the simulations on both model grids. Combined with the data assimilation of the twice-daily McMurdo soundings, the simulations are constrained to be closer to observed fields. The hydrometers that are critical to study are not assimilated and are allowed to develop freely during the simulations.

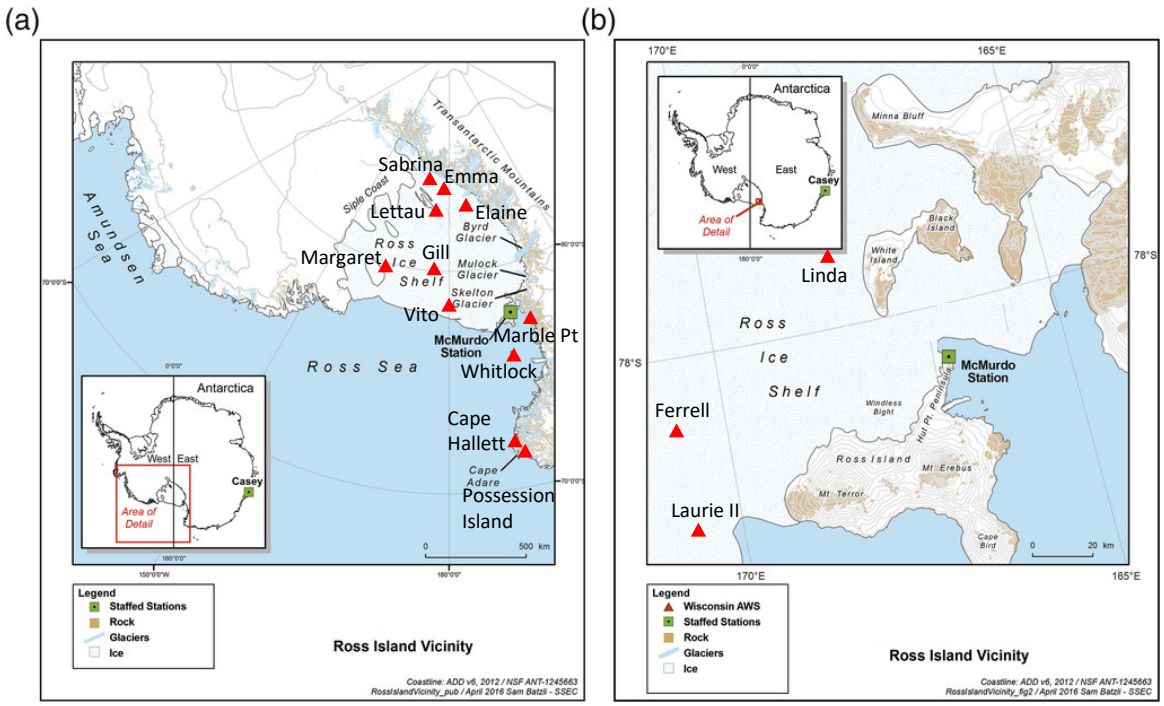

Figure S1. Map of McMurdo, Antarctica and vicinity. (a) The Ross Ice Shelf region, and (b) Ross Island. McMurdo Station is shown by the green square, while red triangles show selected automatic weather stations.

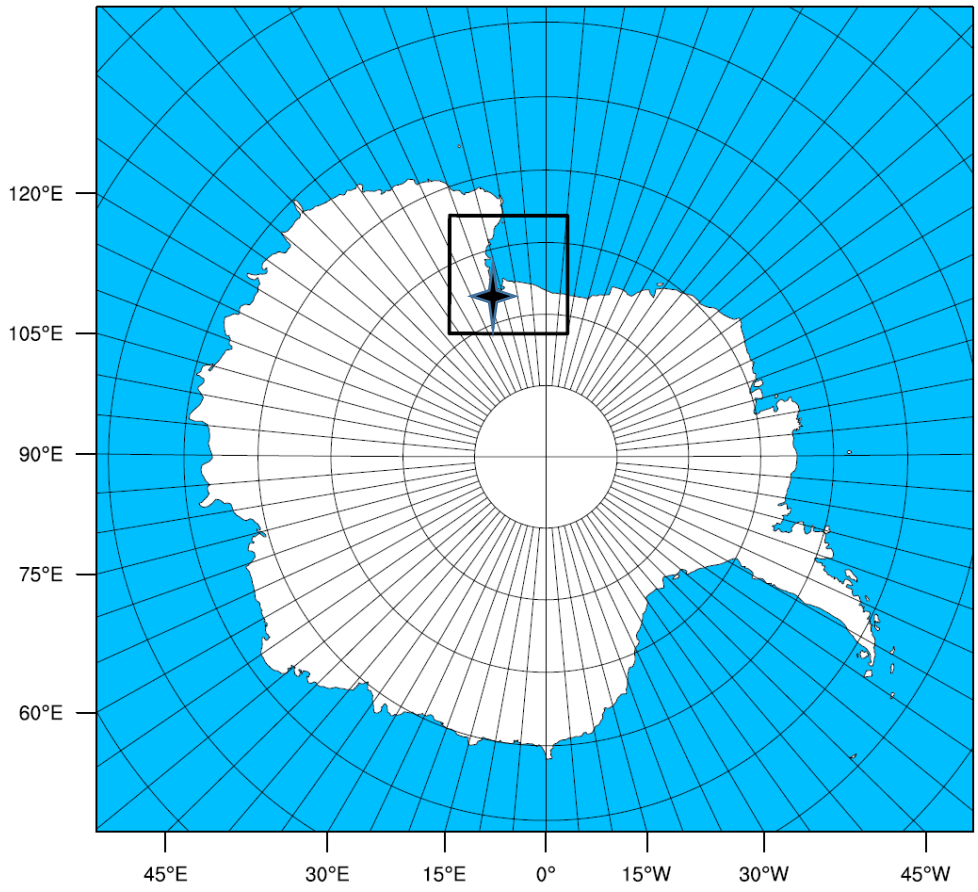

Figure S2. Polar WRF domains. The outer domain has 667 by 628 points and 10-km grid spacing. The nested domain inside the black square has 451 by 451 points and 2-km grid spacing.

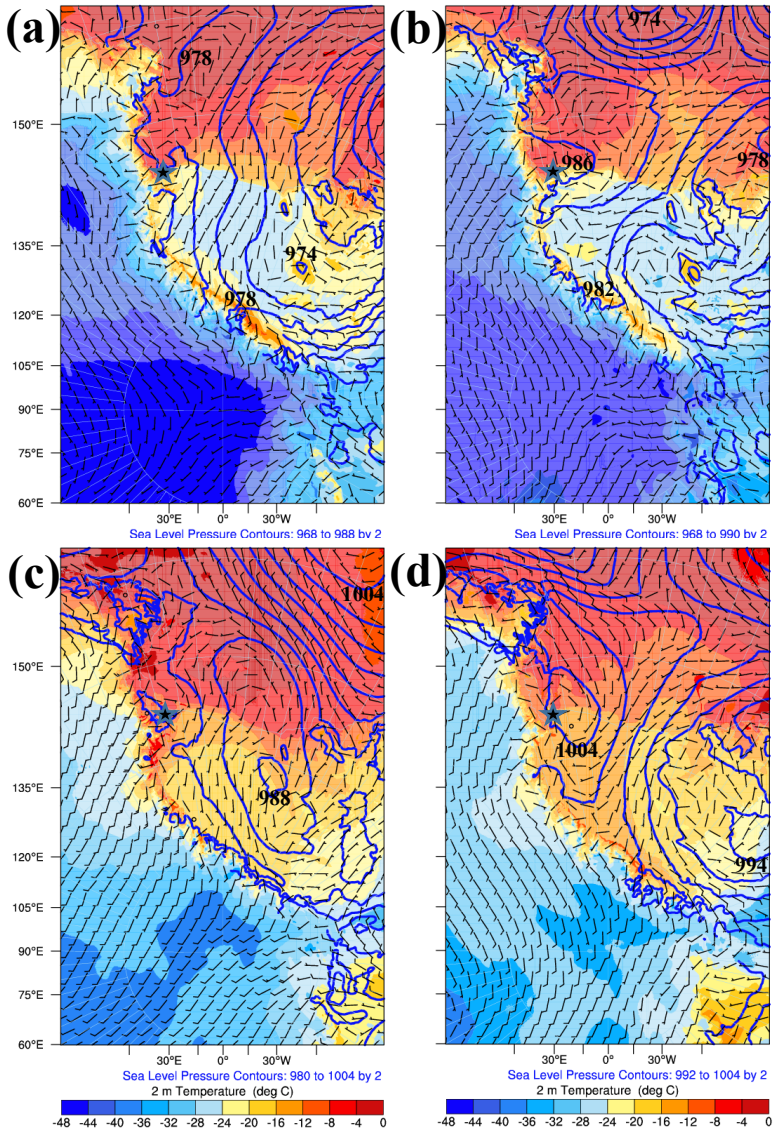

Figure S3. Antarctic Mesoscale Prediction System 6-hr forecast sea level pressure (contours, hPa), 2-m temperature, (colors, °C), and lowest-level wind speed (wind barbs m s^{-1}) at (a) 0600 UTC 8 March 2016, (b) 0600 UTC 11 March 2016, (c) 0600 UTC 9 November 2016), and (d) 12 November 2016. The location of McMurdo is shown by the black star.

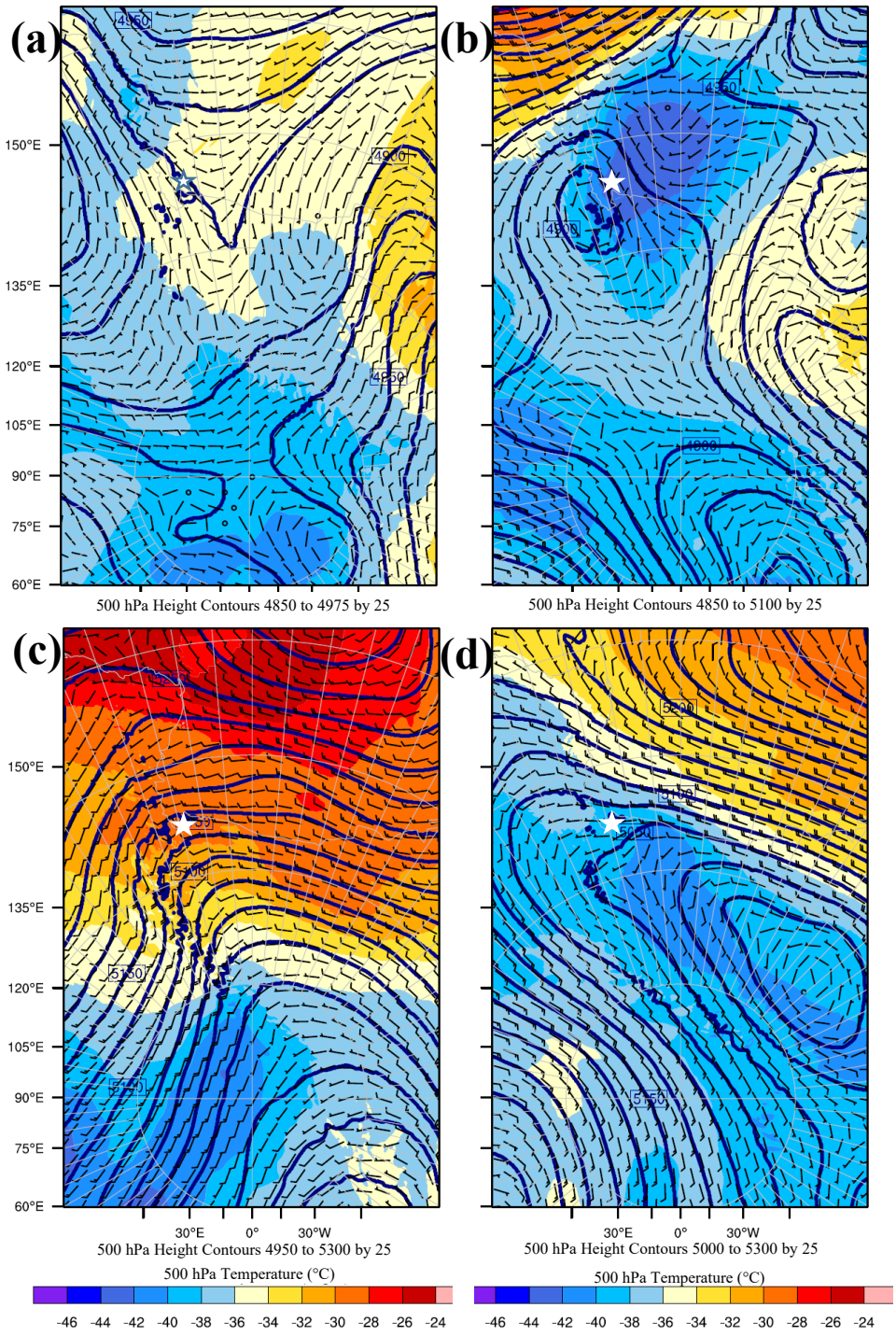

Figure S4. Antarctic Mesoscale Prediction System 6-hr forecast 500 hPa height (contours, m), 500 hPa temperature (colors, ºC), and 500 hPa wind speed (wind barbs, m s^{-1}) at (a) 0600 UTC 8 March 2016, (b) 0600 UTC 11 March 2016, (c) 0600 UTC 9

November 2016, and (d) 0600 UTC 12 November 2016. The location of McMurdo is shown by the star.

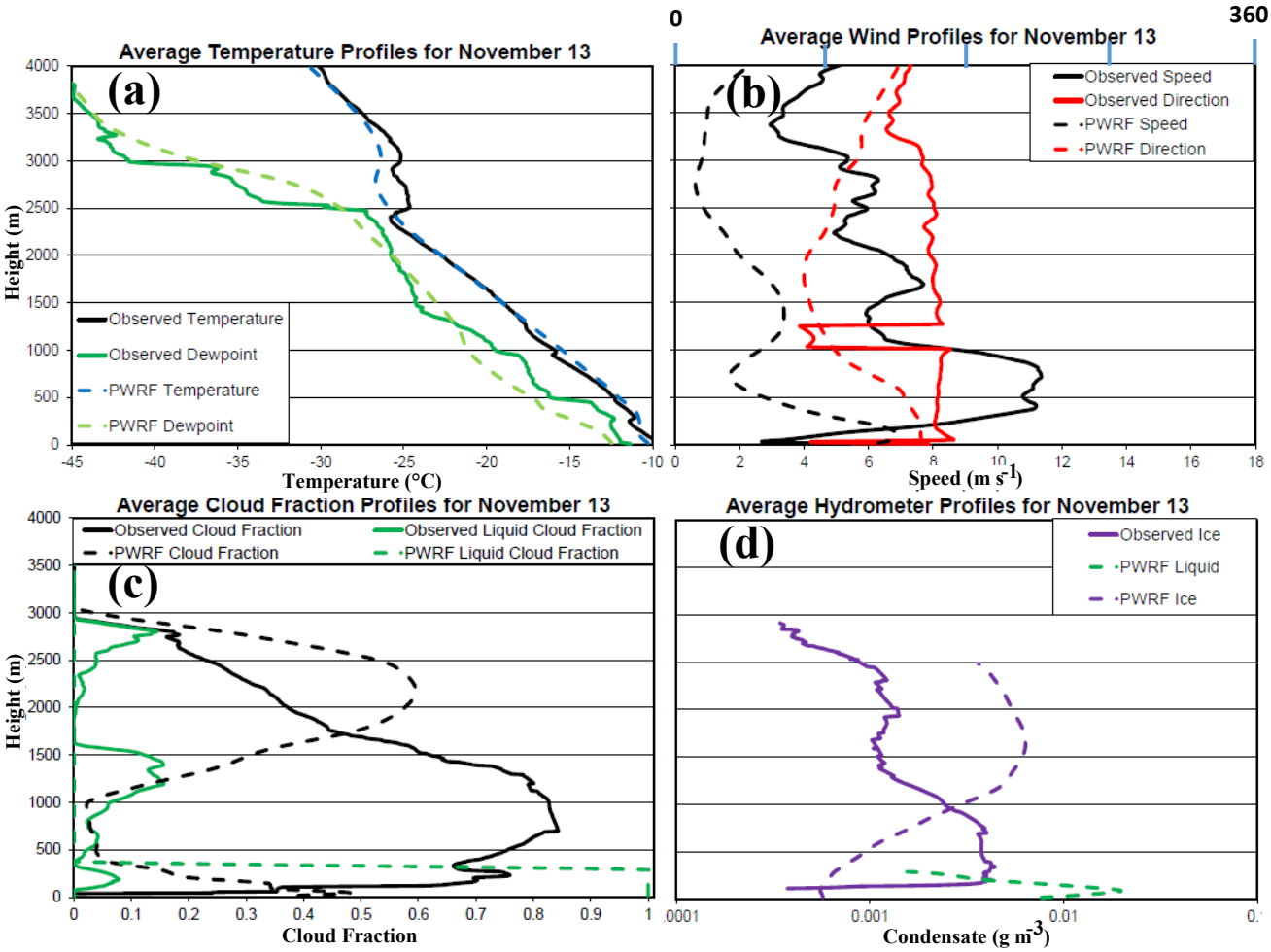

Figure S5. Vertical profiles of observed and simulated fields averaged over 13 November 2016 for (a) temperature (ºC) and dewpoint temperature, (ºC) (b) wind speed (m s^{-1}) and wind direction (degrees), (c) cloud fraction and liquid cloud fraction, and (d) liquid water content and ice water content (g m^{-3}).

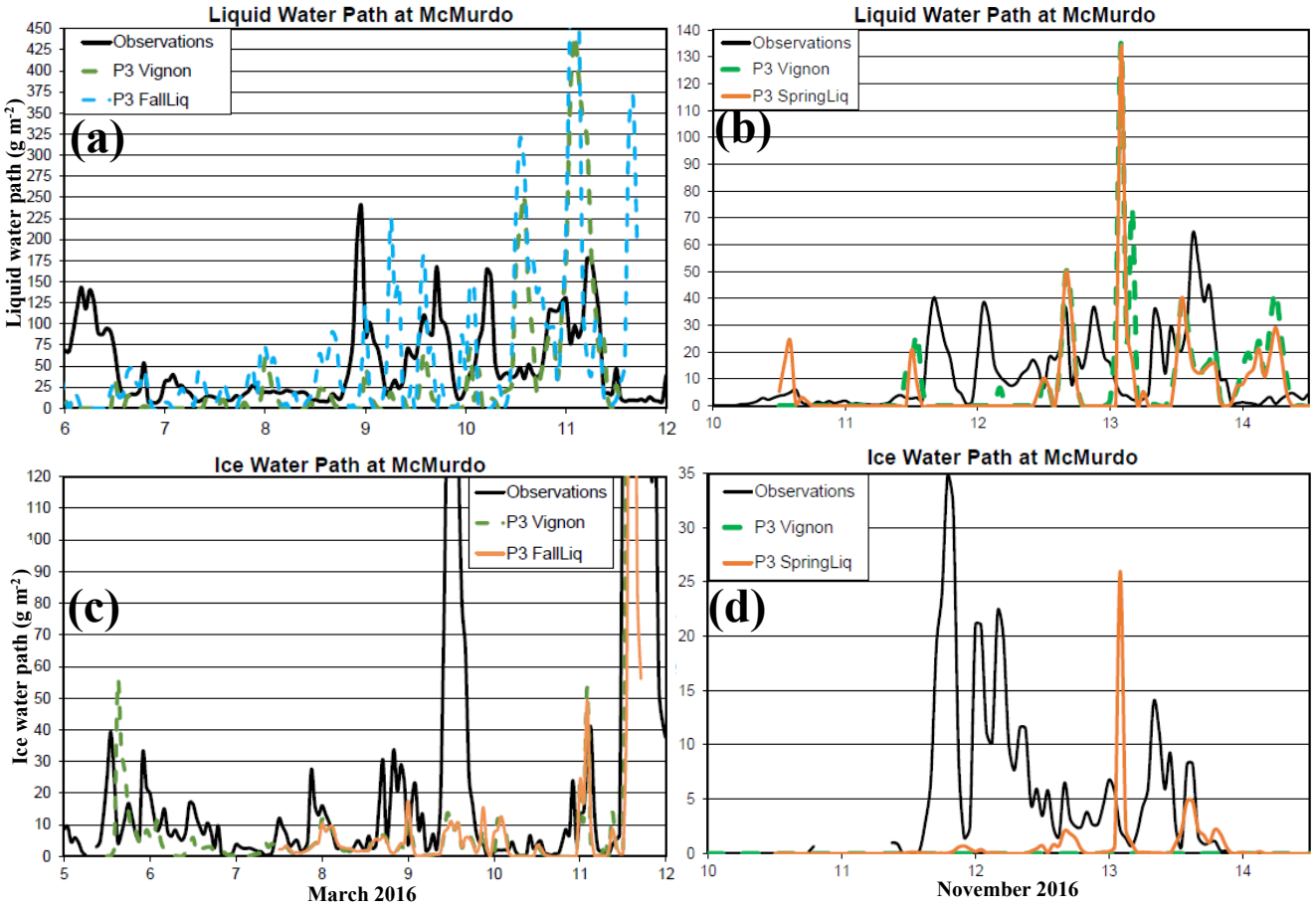

Figure S6. Time series of liquid water path (g m^{-2}) for (a) March 2016, and (b) November 2016, and ice water path (g m^{-2}) for (c) March 2016, and (d) November 2016. Observations are shown by solid black curves, while the Vignon simulation is shown by the green dashed curves. The sensitivity simulations FallLiq and SpringLiq are shown by the light brown curves.

Table S1. Automatic weather stations near McMurdo, Antarctica for data assimilation			
Station	Latitude	Longitude	Surface Height (m)
Cape Hallett	72.19ºS	170.17ºE	1
Elaine	83.10ºS	174.30ºE	62
Emilia	78.47ºS	173.15ºE	51
Emma	84.00ºS	175.01ºW	79
Ferrell	77.84ºS	170.82ºS	45
Gill	79.88ºS	178.57ºW	53
Laurie II	77.50ºS	170.79ºE	34
Lettau	82.49ºS	174.58ºW	39
Manuela	74.95 ºS	163.69 ºE	78
Marble Point II	77.44 ºS	163.76 ºE	111
Marilyn	79.93 ºS	165.56 ºE	62
Margaret	80.00 ºS	165.01ºW	67

Possession Island	71.89ºS	171.22ºE	30
Sabrina	84.25ºS	170.05ºW	88
Schwerdtfeger	79.87ºS	170.15ºE	54
Vito	78.47ºS	177.79ºE	50
Whitlock	76.15ºS	168.40ºE	262

Table S1. Automatic weather stations near McMurdo, Antarctica for data assimilation